

**ORIGINAL  
RESEARCH**

M.P. Wattjes  
G.G. Lutterbey  
J. Gieseke  
F. Träber  
L. Klotz  
S. Schmidt  
H.H. Schild

# Double Inversion Recovery Brain Imaging at 3T: Diagnostic Value in the Detection of Multiple Sclerosis Lesions

**BACKGROUND AND PURPOSE:** To prospectively determine the sensitivity in the detection of multiple sclerosis (MS) lesions by using double inversion recovery (DIR), fluid-attenuated inversion recovery (FLAIR), and T2-weighted turbo spin-echo (T2 TSE) MR imaging at 3T.

**METHODS:** Seventeen patients presenting with a clinically isolated syndrome (CIS) suggestive of MS, 9 patients with definite MS, and 6 healthy control subjects were included. Imaging was performed on a 3T MR system using DIR, FLAIR, and T2 TSE sequences. Lesions were counted and classified according to 5 anatomic regions: infratentorial, periventricular, deep white matter, juxtacortical, and mixed white matter-gray matter. The sensitivity at DIR was compared with the corresponding sensitivity at FLAIR and T2 TSE sequence. The contrast between lesions and normal-appearing gray matter, normal-appearing white matter, and CSF was determined for all sequences.

**RESULTS:** Because of higher lesion-white matter contrast, the DIR showed a higher number of lesions compared with the FLAIR (7% gain,  $P = 0.04$ ) and the T2 TSE (15% gain,  $P = 0.01$ ). The higher sensitivity was also significant for the infratentorial region compared with the FLAIR (56% gain,  $P = 0.02$ ) and the T2 TSE (44% gain,  $P = 0.02$ ). Compared with the FLAIR, no significant changes of the lesion load measurements were observed in the supratentorial brain: slightly higher numbers of periventricular and mixed gray matter-white matter lesions on the DIR were counterbalanced by a slightly reduced sensitivity regarding juxtacortical lesions.

**CONCLUSION:** DIR brain imaging at 3T provides the highest sensitivity in the detection of MS lesions especially in the infratentorial region.

**M**ultiple sclerosis (MS) is the most frequent chronic inflammatory demyelinating disease of the central nervous system (CNS), predominantly affecting the white matter but also parts of the gray matter.<sup>1-4</sup> The diagnosis and disease monitoring of MS is mainly based on MR imaging, which allows the establishment of an early diagnosis of MS within diagnostic criteria.<sup>5-8</sup> Furthermore, MR imaging has a substantial prognostic value in patients with clinically isolated syndromes (CIS) suggestive of MS concerning the prediction of the conversion to definite MS as well as long-term disability and brain atrophy.<sup>9-13</sup>

MR imaging in the diagnosis of MS is performed as a multisequence protocol including T2-weighted, fluid-attenuated inversion recovery (FLAIR) and precontrast and postcontrast T1-weighted sequences.<sup>14,15</sup> The pulse sequences show different sensitivities in the detection of inflammatory brain lesions depending on their anatomic location. FLAIR imaging provides the highest sensitivity in the detection of lesions close to the CSF, such as the juxtacortical and the periventricular white matter, but is less sensitive in the posterior fossa.<sup>16-18</sup> T2-weighted conventional spin-echo or turbo spin-echo (T2 TSE) sequences are known to be more sensitive in the detection of infratentorial lesions but have difficulties detecting juxtacortical lesions.<sup>13,16-18</sup>

Unfortunately, no pulse sequence is available that provides a combination of a high sensitivity for the detection of supratentorial and infratentorial brain lesions in MS patients.

Several years ago, a double inversion recovery pulse sequence (DIR) was introduced.<sup>19</sup> This sequence provides 2 different inversion pulses, which attenuates the CSF as well as the whole white matter, thus achieving a superior delineation between gray and white matter. So far, this sequence has been evaluated at 1.5T in only a limited number of patients with various disease entities, including vascular, inflammatory, malignant, and degenerative CNS diseases.<sup>20,21</sup>

The aim of our study was to evaluate the diagnostic value of a DIR sequence at high-field MR imaging operating at 3T in the detection of MS lesions by prospectively comparing DIR with FLAIR and T2-weighted pulse sequences.

## Methods

### Patients and Healthy Control Subjects

Twenty-six patients were prospectively included in this intraindividual comparative study. Seventeen patients presented with a CIS suggestive of MS (median age, 40 years; range, 19–56 years; mean disease duration, 5 months; range, 0–8 months; median Expanded Disability Status Scale [EDSS], 1; range, 0–4). Nine patients had a relapsing-remitting course of multiple sclerosis (median age, 36 years; range, 23–47 years; mean disease duration, 51 months; range, 3–189 months; median EDSS, 1.5; range, 0–6). Among the patients presenting with CIS, 10 patients presented with unilateral optic neuritis, 3 patients with spinal cord syndromes, 3 patients with brain stem syndromes, and one patient with a polysymptomatic CIS. In addition, 6 healthy control subjects (3 men, 3 women; median age, 28 years) were

Received January 12, 2006; accepted after revision March 8.

From the Departments of Radiology/Neuroradiology (M.P.W., G.G.L., J.G., F.T., H.H.S.) and Neurology (L.K., S.S.), University of Bonn, Bonn, Germany; and Philips Medical Systems (J.G.), Best, the Netherlands.

This work was presented on the 4th International Symposium on Highfield MRI in Clinical Applications; September 9–10, 2005; Bonn, Germany.

Address correspondence to Mike Peter Wattjes, MD, Department of Radiology, University of Bonn, Sigmund-Freud-Str 25, 53105 Bonn, Germany; e-mail: mike.wattjes@ukb.uni-bonn.de

**Table 1: MRI sequence parameters**

Parameter	DIR	FLAIR	T2 TSE
Field of view (mm)	230	230	230
Matrix	256	256	256
Section thickness (mm)	5	5	5
Measured voxel size (mm)	0.90/0.90/5	0.90/0.90/5	0.90/0.90/5
SENSE factor	1.5	1.6	
Turbo factor	13	38	16
Repetition time (ms)	11000	12000	4100
Echo time (ms)	29	140	100
Inversion time (ms)	3400/325*	2850	
Number of signals averaged	1	1	1
Bandwidth/pixel (Hz)	277.9	287	184.3
Acquisition time (minutes:seconds)	3:18	4:00	2:19

**Note:**—DIR indicates double inversion recovery; FLAIR, fluid-attenuated inversion recovery; T2 TSE, T2-weighted turbo spin-echo; SENSE sensitivity encoding.

\* The long inversion time  $TI_1$  (3400 ms) is defined as the interval between the first 180° inversion pulse and the 90° excitation pulse. The short inversion time  $TI_2$  (325 ms) is defined as the interval between the second 180° inversion pulse and the 90° excitation pulse.

included. All patients were selected and referred by the MS outpatient center, Department of Neurology, University Hospital Bonn. Our local ethics review board approved the study protocol. All patients gave written informed consent before the examination. Regarding the patients presenting with CIS the neurologic work-up included the CSF parameters (including the assessment of cellularity, protein level, intrathecal IgG synthesis, and oligoclonal bands by isoelectric focusing) and visual evoked potentials. All other differential diagnosis of CIS and MS including vascular, malignant, infectious, and other immunological CNS diseases were excluded by appropriate tests.

### MR Imaging

The MR examinations were performed at a 3T whole-body MR system (Gyrosan Intera Achieva; Philips Medical Systems, Best, the Netherlands) using an 8-element phased array sensitivity-encoding (SENSE) head coil. The MR system was equipped with gradients achieving a maximum slew rate of 200 mT/m/ms and a maximum strength of 80 mT/m. The imaging protocol included 24 contiguous axial sections of a T2 TSE, FLAIR, and DIR. In the DIR sequence, 2 different inversion pulses were applied. Both inversion times,  $TI_1$  and  $TI_2$  in our DIR sequence, were defined as the intervals between the respective 180° inversion pulse and the 90° excitation pulse, which means that the 2 inversion pulses are separated by  $TI_1 - TI_2$ . These inversion times were calculated according to the formulas given by Turetschek et al<sup>21</sup> and optimized in healthy volunteers for a simultaneous CSF suppression and attenuation of the white matter signal intensity. Because of the additional second inversion pulse, the first inversion time of the DIR sequence has to be prolonged compared with the TI of the FLAIR sequence to provide a sufficient CSF attenuation. The detailed sequence parameters are given in Table 1. All sequences were performed with identical anatomic positions and geometric and resolution parameters using a measured voxel size of 5/0.9/0.9 mm. The scan orientation and repositioning was performed according to the guidelines of the Consortium of MS Centers.<sup>14</sup>

### Image Analysis

Two radiologists interpreted the images by consensus after the images were transferred to a workstation (Easy Vision; Philips Medical Systems). The images of the different pulse sequences were separated and presented in a randomized order. Both readers were blinded to the clinical presentation and the results of the paraclinical tests. High-signal-intensity brain lesions with a size of >3 mm were counted and

classified according to their location as infratentorial, periventricular white matter, juxtacortical white matter, mixed white matter-gray matter, or deep white matter lesions. All DIR, FLAIR, and T2 TSE images of the healthy control subject and patients were evaluated for artifacts.

The contrast ratios of all 3 pulse sequences were determined from the respective mean values of the contrast between lesions and normal-appearing gray matter (NAGM), lesions, and normal-appearing white matter (NAWM) as well as between lesions and CSF. The contrast was defined as  $|SI_1 - SI_2|/(SI_1 + SI_2)$ .  $SI_1$  was defined as the signal intensity of the lesions and  $SI_2$  as the signal intensity of the NAWM, NAGM, or CSF, respectively. The signal intensity measurements were obtained using the region-of-interest analysis. The regions were placed in the lesions, the NAWM, NAGM, and CSF. The contrast measurements between lesions and the NAWM were performed separately in the infratentorial, periventricular, juxtacortical, and deep white matter regions. Signal-to-noise ratio (SNR) and contrast-to-noise ratio (CNR) could not be calculated because of the automatic implementation of the constant level appearance (CLEAR) algorithm for signal intensity homogeneity correction of the images obtained by the 8-element SENSE head coil.

### Statistical Analysis

The analysis of brain lesions on the different pulse sequences was performed lesion- and patient-wise. The statistical differences in both analyses were assessed using the Wilcoxon test for matched pairs. The relative comparison of the numbers of lesions on DIR versus FLAIR and T2 TSE, respectively, was expressed as percentage gain or a loss in the number of detected brain lesions.

The significances of contrast differences between the 3 sequences were assessed using the Wilcoxon test for matched pairs. All calculations were performed by the SPSS software package (SPSS, Chicago, Ill). *P* values  $\leq 0.05$  were considered as statistically significant.

## Results

### Healthy Control Subjects

Besides discrete high-signal-intensity changes caused by CSF effusion effects in the periventricular white matter and in the periaqueductal area, no unspecific white matter or gray matter abnormalities were identified on the T2 TSE, FLAIR, and DIR images.

The DIR images showed slightly more artifacts in the posterior fossa in terms of vascular and flow artifacts than the corresponding FLAIR and T2 TSE images. Both readers found that those artifacts did not impair the diagnostic quality compared with the FLAIR and T2 TSE images. The attenuation of the CSF was sufficient and similar on the FLAIR and DIR images.

### Patients with CIS and MS

The detailed results of the lesion load analysis are given in Table 2. In our patients with suspected or definite MS, 201 lesions could be identified with T2 TSE, 216 lesions with FLAIR, and 232 lesions with DIR. This higher overall detection rate at DIR was significant compared with both T2 TSE ( $P = 0.01$ ) and FLAIR ( $P = 0.04$ ) MR imaging. Considering the different anatomic regions, the higher detection rate of the DIR imaging was significant for the detection of infratentorial lesions compared with the T2 TSE ( $P = 0.02$ ) and FLAIR ( $P =$

**Table 2: Analysis of the lesion load measurement and relative comparisons of the DIR versus the FLAIR and T2-weighted TSE sequences**

Region	DIR*	FLAIR*	T2TSE*	Relative Comparison (%) <sup>†</sup>			
				DIR/FLAIR	P Value <sup>‡</sup>	DIR/T2 TSE	P Value <sup>‡</sup>
Infratentorial	39	25	27	56	0.02	44	0.02
Periventricular	85	81	76	5	0.16	12	0.03
Juxtacortical	54	57	49	-6	0.08	10	0.18
Mixed WM-GM	21	18	14	17	0.32	50	0.06
Deep WM	35	36	35	-3	0.32	0	1
Total	232	216	201	7	0.04	15	0.01

**Note:**—GM indicates gray matter; WM, white matter; DIR, double inversion recovery; FLAIR, fluid-attenuated inversion recovery; T2 TSE, T2-weighted turbo spin-echo.

\* Data are numbers of detected lesions.

<sup>†</sup> Data are relative differences in the numbers of detected lesions expressed as percentages of lesion numbers identified with DIR imaging compared with the corresponding FLAIR and T2 TSE imaging.

<sup>‡</sup> P value was obtained from the patient-wise analysis by Wilcoxon analysis for matched pairs indicating that more or fewer patients showed higher lesion load measurement with DIR imaging in comparison with the corresponding FLAIR or T2 TSE imaging.

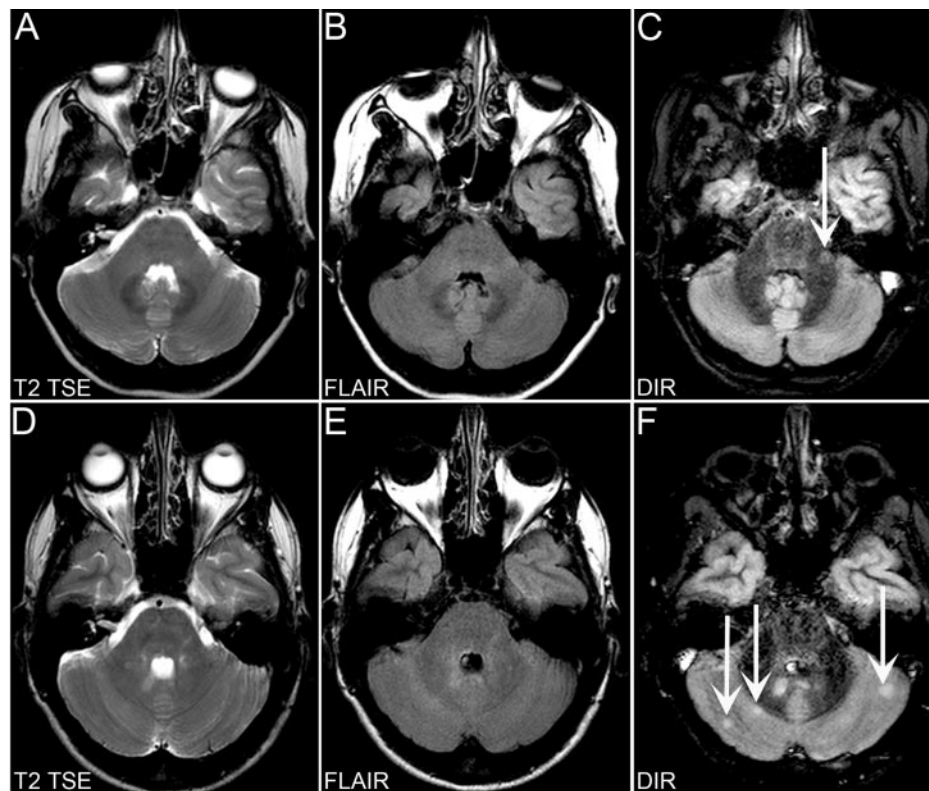


**Fig 1.** Transverse T2-weighted TSE, FLAIR, and DIR image examples documenting the higher sensitivity of DIR in the detection of inflammatory brain lesion in the infratentorial brain.

*Top row (A–C),* A 36-year-old woman presenting with a polysymptomatic CIS. A sharp delineated inflammatory lesion in the left pedunculus cerebelli (*arrow*) can be clearly identified on the DIR image but not on the corresponding sections of the T2 TSE and FLAIR sequences.

*Bottom row (D–F),* A 23-year-old man presenting with optic neuritis of the left eye. Compared with the T2 TSE and FLAIR images, more lesions in both hemispheres of the cerebellum (*arrows*) can be identified on the DIR image. Moreover, those lesions identified on all 3 sequences were better delineated on DIR compared with the corresponding T2 TSE and FLAIR images.

0.02) sequence (Fig 1). The DIR detected 56% more infratentorial lesions compared with the FLAIR and 44% compared with the T2 TSE sequence. Regarding the supratentorial brain, higher detection rates were observed using DIR imaging compared with the T2 TSE imaging. This was statistically significant for the periventricular white matter ( $P = 0.03$ ). The relative gain of detected lesions when using DIR imaging compared with T2 TSE imaging was 66% regarding the periventricular region, 10% regarding the juxtacortical region, and 50% regarding the mixed white matter-gray matter region. Compared with FLAIR imaging, DIR imaging showed a similar sensitivity in the detection of supratentorial MS lesions (Fig 2). FLAIR imaging depicted slightly more lesions in the juxtacortical white matter (relative gain of 6%) and deep white matter (relative gain of 3%), whereas DIR imaging identified slightly more lesions in the mixed white matter-gray matter (relative gain of 17%) and periventricular white matter (relative gain of 5%). None of these minor differences in the lesion load measurement reached statistical significance in the pa-

tient-wise analysis. Figure 3 gives examples of the higher detection rate of mixed white matter-gray matter lesions on the DIR images.

#### Image Contrast Measurements

The areas of the region of interest had a mean size of 65 mm<sup>2</sup> (SD, 23 mm<sup>2</sup>; range, 34–107 mm<sup>2</sup>) for the NAGM, 100 mm<sup>2</sup> (SD, 37 mm<sup>2</sup>; range, 48–178 mm<sup>2</sup>) for the CSF, 101 mm<sup>2</sup> (SD, 37 mm<sup>2</sup>; range, 36–161 mm<sup>2</sup>) for the NAWM, and 74 mm<sup>2</sup> (SD, 39 mm<sup>2</sup>; range, 24–190 mm<sup>2</sup>) for the lesions. The results of the contrast measurements of DIR, FLAIR, and T2 TSE imaging are listed in Table 3.

The contrast between lesions and the NAWM was higher on the DIR images compared with the corresponding T2 TSE and FLAIR sequences in every anatomic region (DIR compared with the T2 TSE and FLAIR sequences regarding the juxtacortical, periventricular, and deep white matter region,  $P = 0.05$ ; DIR compared with the T2 TSE and FLAIR sequences regarding the infratentorial brain,  $P = 0.03$ ). The



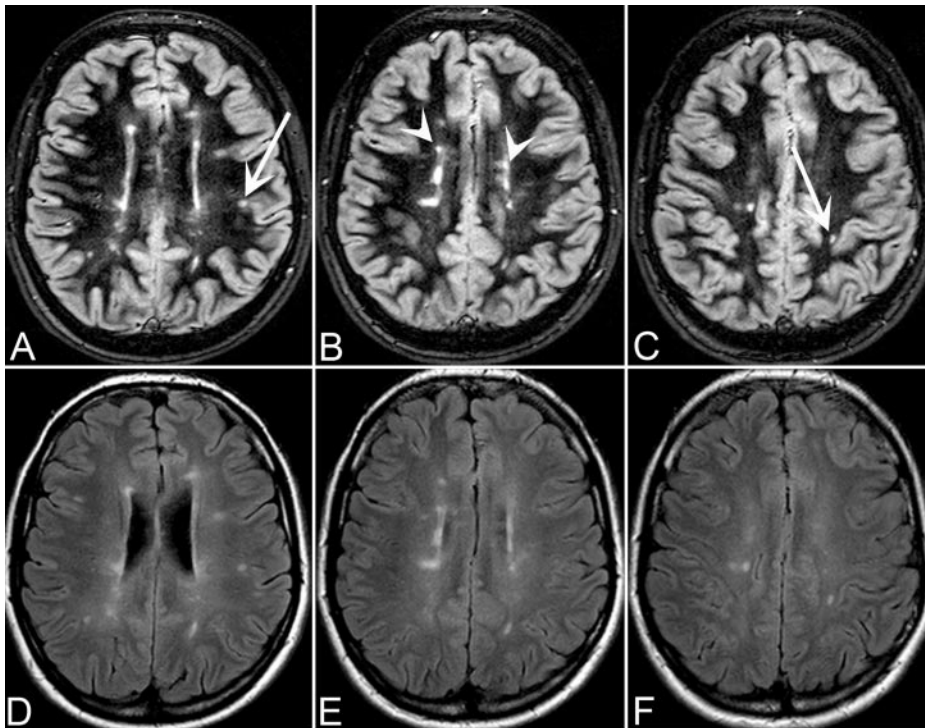


**Fig 2.** Transverse FLAIR (*bottom row*) and DIR (*top row*) sections of the supratentorial brain. The inflammatory lesions have a more sharp delineated appearance on the DIR compared with the corresponding FLAIR images. Despite a minor contrast between lesions and the normal-appearing gray matter, DIR showed a high sensitivity in the detection of juxtacortical and mixed white matter-gray matter lesions (*arrows*). A differentiation between juxtacortical and mixed white matter-gray matter lesions is much easier on the DIR than on the FLAIR images. Regarding the periventricular white matter, the lesions are easier to identify on the DIR compared with the FLAIR images (*open arrows*).

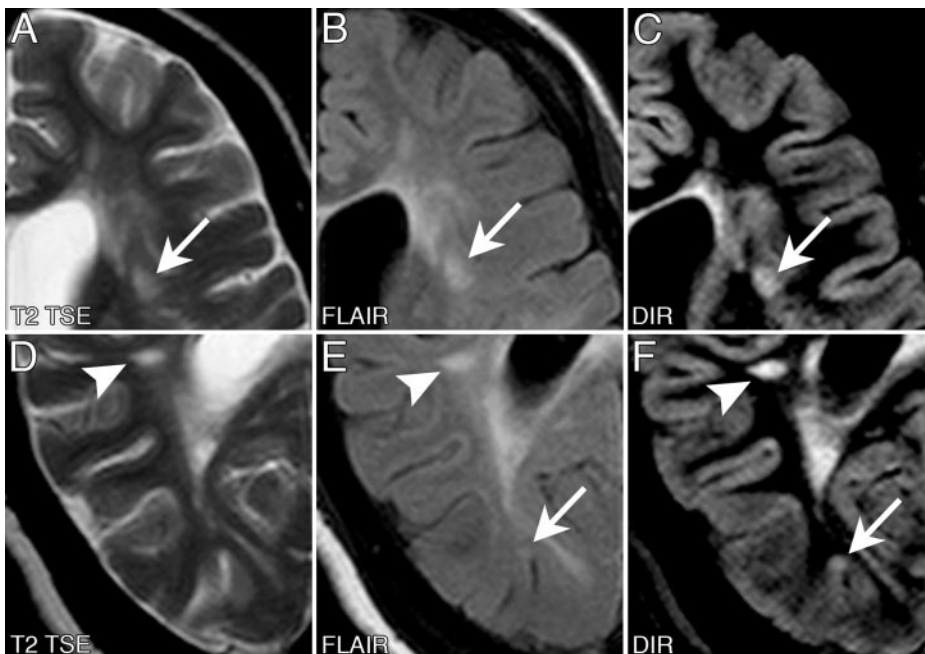


**Fig 3.** Image examples of the improved detection of mixed white matter-gray matter lesions on the DIR pulse sequence. These images were obtained from a 40-year-old woman with a relapsing-remitting course of MS (disease duration, 165 months; EDSS, 6) presenting with a high lesion load on the MR imaging, including mixed white matter-gray matter lesions. *Top row*, an example of different classifications of a lesion using different pulse sequences. A lesion (*arrow*) was prospectively classified as a juxtacortical lesion on the T2 TSE and FLAIR images. Because of the better delineation of the white and gray matter on the DIR image, this lesion had to be reclassified into a mixed white matter-gray matter lesion. *Bottom row*, an example of the higher conspicuity of a cortical lesion (*arrow*) on the DIR image that was not prospectively identified on the corresponding T2 TSE and FLAIR images. Another lesion (*open arrow*) could be easily identified and categorized on the DIR image as a pure juxtacortical lesion without touching the cortex.

contrast between the lesion and the CSF was also superior using DIR imaging compared with T2 TSE and FLAIR imaging ( $P = 0.05$  compared with both T2 TSE and FLAIR imaging). Regarding the contrast between lesions and the NAGM, FLAIR, and T2 TSE imaging showed slightly higher contrast values that did not reach statistical significance (FLAIR compared with DIR,  $P = 0.72$ ; T2 TSE compared with DIR,  $P = 0.29$ ).

### Discussion

Despite new emerging MR techniques in the diagnostic work-up of patients with suspected or definite MS, including MR spectroscopy and diffusion tensor imaging,<sup>22,23</sup> the diag-

nosis of MS is still based mainly on conventional multi-sequence MR imaging protocols.<sup>5,9,10,14</sup> Over the past few years, inversion recovery pulse sequences, such as FLAIR sequences, have increasingly been incorporated into imaging protocols and guidelines for the detection of inflammatory brain lesions. Because of the attenuation of the CSF, FLAIR imaging is highly sensitive in the detection of supratentorial brain lesions, especially in the juxtacortical and periventricular white matter. A more recently established double inversion recovery imaging technique by using a combination of 2 inversion pulses provides a sufficient attenuation of both CSF and the NAWM. Two major studies focused on the diagnostic value of this type of sequence concerning different applica-

**Table 3: Contrast measurements of the DIR, FLAIR, and T2 TSE sequences**

	Contrast*			Contrast Ratio	
	DIR	FLAIR	T2 TSE	DIR vs FLAIR†	DIR vs T2 TSE†
Lesion/NAWM					
Infratentorial	0.460 ± 0.125	0.137 ± 0.060	0.181 ± 0.067	3.36	2.54
Periventricular	0.788 ± 0.098	0.253 ± 0.070	0.341 ± 0.085	3.11	2.31
Deep WM	0.720 ± 0.066	0.217 ± 0.047	0.298 ± 0.070	3.32	2.42
Juxtacortical	0.772 ± 0.110	0.253 ± 0.045	0.335 ± 0.047	3.05	2.30
Lesion/NAGM	0.190 ± 0.097	0.198 ± 0.064	0.213 ± 0.076	0.96	0.89
Lesion/CSF	0.832 ± 0.103	0.653 ± 0.243	0.201 ± 0.101	1.27	4.14

**Note:**—NAWM indicates normal-appearing white matter; WM, white matter; NAGM, normal-appearing grey matter; DIR, double inversion recovery; FLAIR, fluid-attenuated inversion recovery; T2 TSE, T2-weighted turbo spin-echo.

\* Data are presented as means ± SD.

† Data are the contrast values of the DIR sequence in relative comparison with the corresponding contrast value of the FLAIR and T2 TSE sequence.

tions in clinical neuroimaging, including vascular, infectious, neoplastic, and inflammatory CNS diseases.<sup>20,21</sup> Although the results of these studies were quite promising, especially regarding pathologies in the infratentorial brain region, DIR brain imaging was not established as a standard sequence within the clinical routine because of its relatively long acquisition time and propensity to CSF pulsation artifacts.<sup>21</sup>

The experiences of DIR brain imaging in the past are limited to magnetic field strengths up to 1.5T. Higher magnetic field strengths are providing an almost linear increase of the signal-to-noise ratio, and they enable us to invest these higher signal intensity values in faster imaging techniques, including parallel imaging protocols.<sup>24,25</sup> In addition, high-field MR imaging in patients with MS provides a significantly higher sensitivity in the detection of inflammatory brain lesions compared with lower magnetic field strengths up to 1.5T, leading to diagnostic relevance in terms of diagnostic imaging criteria.<sup>26-28</sup> Therefore, 3T MR imaging is a promising method to achieve DIR imaging with an acceptable acquisition time in combination with a high sensitivity in the detection of MS lesions.

In this study, we introduced a DIR pulse sequence at 3T, which allows a sufficient attenuation of the CSF and the NAWM. This achieved an improved contrast ratio and delineation between gray and white matter compared with the corresponding T2 TSE and FLAIR imaging. Regarding the detection of MS lesions, DIR imaging provides higher contrast ratios between lesions and the NAWM in all anatomic locations compared with FLAIR and T2 TSE imaging. This resulted in a high sensitivity in the detection of supratentorial brain lesions that was similar to the “gold standard” of FLAIR imaging. However, DIR at 3T showed a slightly lower sensitivity in the detection of lesions in the juxtacortical white matter that was counterbalanced by a higher lesion load measurement concerning the mixed white matter-gray matter lesions, similar to results at 1.5T.<sup>29</sup> Concerning white matter-gray matter lesions, this higher sensitivity at 3T is not as strongly developed compared with the results at 1.5T<sup>29</sup> using a 3D DIR sequence. However, this finding is quite interesting because the contrast between lesions and the NAGM of the DIR is almost similar to the contrast at the FLAIR and T2 TSE sequences. The major reason for these different detection rates in the juxtacortical white matter and the mixed white matter-gray matter lesions is the sharp delineation between gray and white matter on the DIR, which allows a very stringent differentiation

between purely juxtacortical lesions and lesions already touching the cortical area. Therefore, some of the lesions initially identified as juxtacortical lesions on the FLAIR and T2 TSE have to be categorized as mixed white matter-gray matter lesions on the DIR, leading to lower numbers of juxtacortical and higher numbers of mixed white matter-gray matter lesions. In addition, in concordance with the results at 1.5T, the contrast measurements between lesions and the NAGM show a relatively high variation.<sup>21</sup> At the time of the zero crossing of the CSF and NAWM magnetization on the DIR, the magnetization of the NAGM is also decreased (in absolute terms), leading to a signal intensity attenuation in the magnitude images and, therefore, in some cases, to a better lesion conspicuity within the NAGM. Since recently performed histopathologic studies revealed that intracortical lesions are frequently observed in MS patients, the detection of those intracortical lesions is becoming increasingly important and is therefore of diagnostic and prognostic interest.<sup>2,4,30</sup>

In contrast to almost similar detection rates in the supratentorial brain, DIR identified significantly more inflammatory lesions in the infratentorial brain even compared with the T2 TSE sequence, which is still the diagnostic “gold standard” in the infratentorial region at higher magnetic field strengths.<sup>31</sup> Because a higher infratentorial lesion load is important for the prediction of long-term disability in patients with the first clinical event suggestive of MS, this result has major prognostic relevance.<sup>12</sup> A better detection of infratentorial pathologies on DIR has already been observed at 1.5T, leading to the conclusion that this has primarily not been influenced by the higher field strength in our study. However, the relatively short echo time of 29 ms pronounces a more proton density-weighted effect of our DIR sequence. This might be partially responsible for the impressive high detection rate and lesion contrast in the infratentorial brain region.<sup>16</sup>

Although artifacts in the posterior fossa, such as vascular and flow artifacts, were slightly pronounced on DIR imaging, the higher sensitivity in the detection of infratentorial lesions was not influenced by a possible misinterpretation of artifacts for lesions. Because infratentorial lesions could not be identified on DIR imaging in the healthy control subjects, a misinterpretation of artifacts for infratentorial lesions is even more implausible, though those healthy control subjects were not exactly age-matched to both patient groups.

## Conclusion

High-field MR imaging at 3T allows the establishment of a fast and accurate DIR imaging protocol. In patients with suspected or definite MS, DIR brain imaging at 3T provides the highest overall sensitivity in the detection of MS lesions compared with the standard pulse sequences of FLAIR and T2-weighted TSE. This higher sensitivity is especially obvious in the infratentorial region and is therefore of major prognostic relevance.

## Acknowledgments

We thank Hanno Schimikowski for the help establishing the figures and Renate Blömer for the technical assistance. We also thank Jeroen J. G. Geurts, PhD, for providing his expertise in gray matter pathology and DIR imaging in multiple sclerosis.

## References

1. Trapp BD, Peterson J, Ransohoff RM, et al. Axonal transection in the lesions of multiple sclerosis. *N Engl J Med* 1998;338:278–85
2. Kidd D, Barkhof F, McConnell R, et al. Cortical lesions in multiple sclerosis. *Brain* 1999;122:17–26
3. Ge Y, Grossman RI, Udupa JK, et al. Magnetization transfer ratio histogram analysis of grey matter in relapsing-remitting multiple sclerosis. *AJNR Am J Neuroradiol* 2001;22:470–75
4. Geurts JJG, Bo L, Pouwels PJW, et al. Cortical lesion in multiple sclerosis: combined postmortem MR imaging and histopathology. *AJNR Am J Neuroradiol* 2005;26:572–77
5. Polman CH, Reingold SC, Edan G, et al. Diagnostic criteria for multiple sclerosis: 2005 revisions to the “McDonald Criteria”. *Ann Neurol* 2005;58:840–46
6. Dalton CM, Brex PA, Miszkal KA, et al. Application of the new McDonald criteria to patients with clinically isolated syndromes suggestive of multiple sclerosis. *Ann Neurol* 2002;52:47–53
7. Tintoré M, Rovira A, Río J, et al. New diagnostic criteria for multiple sclerosis. Application in first demyelinating episode. *Neurology* 2003;60:27–30
8. Miller DH, Filippi M, Fazekas F, et al. Role of magnetic resonance imaging within diagnostic criteria for multiple sclerosis. *Ann Neurol* 2004;56:273–78
9. Barkhof F, Filippi M, Miller DH, et al. Comparison of MRI criteria at first presentation to predict conversion to clinically definite multiple sclerosis. *Brain* 1997;120:2059–69
10. Tintoré M, Rovira A, Martínez MJ, et al. Isolated demyelinating syndromes: comparison of different MR imaging criteria to predict conversion to clinically definite multiple sclerosis. *AJNR Am J Neuroradiol* 2000;21:702–06
11. Barkhof F, Rocca M, Francis G, et al. Validation of diagnostic magnetic resonance imaging criteria for multiple sclerosis and response to interferon  $\beta$ 1a. *Ann Neurol* 2003;53:718–24
12. Minneboo A, Barkhof F, Polman CH, et al. Infratentorial lesions predict long-term disability in patients with initial findings suggestive of multiple sclerosis. *Arch Neurol* 2004;61:217–21
13. Bakshi R, Ariyaratana S, Benedict RH, et al. Fluid-attenuated inversion recovery magnetic resonance imaging detects cortical and juxtacortical multiple sclerosis lesions. *Arch Neurol* 2001;58:742–48
14. Simon JH, Li D, Traboulsee A, et al. Standardized MR imaging protocol for multiple sclerosis: Consortium of MS Centers consensus guidelines. *AJNR Am J Neuroradiol* 2006;27:455–61
15. Filippi M, Falini A, Arnold DL, et al. Magnetic resonance techniques for the in vivo assessment of multiple sclerosis pathology: consensus report of the white matter study group. *J Magn Reson Imaging* 2005;21:669–75
16. Frohman EM, Zhang H, Kramer PD, et al. MRI characteristics of MLF in MS patients with chronic internuclear ophthalmoparesis. *Neurology* 2001;57:762–68
17. Gawne-Cain ML, O’Riordan JI, Thompson AJ, et al. Multiple sclerosis lesion detection in the brain: a comparison of fast fluid-attenuated inversion recovery and conventional T2-weighted dual spin echo. *Neurology* 1997;49:364–70
18. Youstry TA, Filippi M, Becker C, et al. Comparison of MR pulse sequences in the detection of multiple sclerosis lesions. *AJNR Am J Neuroradiol* 1997;18:959–63
19. Redpath TW, Smith FW. Technical note: use of a double inversion recovery pulse sequence to image selectively grey or white brain matter. *Br J Radiol* 1994;67:1258–63
20. Bedell BJ, Narayana PA. Implementation and evaluation of a new pulse sequence for rapid acquisition of double inversion recovery images for simultaneous suppression of white matter and CSF. *J Magn Reson Imaging* 1998;8:544–47
21. Turetschek K, Wunderbaldinger P, Bankier AA, et al. Double inversion recovery imaging of the brain: initial experience and comparison with fluid attenuated inversion recovery imaging. *Magn Reson Imaging* 1998;16:127–35
22. He J, Inglesse M, Li BS, et al. Relapsing-remitting multiple sclerosis: metabolic abnormality in nonenhancing lesions and normal-appearing white matter at MR imaging: initial experience. *Radiology* 2005;234:211–17
23. Filippi M, Cercignani M, Inglesse M, et al. Diffusion tensor magnetic resonance imaging in multiple sclerosis. *Neurology* 2001;56:304–11
24. Schick F. Whole-body MRI at high field: technical limits and clinical potential. *Eur Radiol* 2005;15:639–44
25. Frayne R, Goodyear BG, Dickhoff P, et al. Magnetic resonance imaging at 3.0 Tesla: challenges and advantages in clinical neurological imaging. *Invest Radiol* 2003;38:385–402
26. Keiper MD, Grossmann RI, Hirsch JA, et al. MR identification of white matter abnormalities in multiple sclerosis: a comparison between 1.5T and 4T. *AJNR Am J Neuroradiol* 1998;19:1489–93
27. Sicotte NL, Voskuhl RR, Bouvier S, et al. Comparison of multiple sclerosis lesions at 1.5 and 3.0T. *Invest Radiol* 2003;38:423–27
28. Wattjes MP, Harzheim M, Kuhl CK, et al. Does high-field MRI have an influence on the classification of patients with clinically isolated syndromes according to current diagnostic magnetic resonance imaging criteria for multiple sclerosis? *AJNR Am J Neuroradiol* 2006;27:1794–98.
29. Geurts JJG, Pouwels PJW, Uitendhaag BMJ, et al. Intracortical lesions in multiple sclerosis: improved detection with double inversion-recovery MR imaging. *Radiology* 2005;236:254–60
30. Bo L, Vedeler CA, Nyland H, et al. Intracortical lesions are not associated with increased lymphocyte infiltration. *Mult Scler* 2003;9:323–31
31. Wattjes MP, Lutterbey G, Harzheim M, et al. Imaging of inflammatory lesions at 3.0 Tesla in patients with clinically isolated syndromes suggestive of multiple sclerosis: a comparison of fluid-attenuated inversion recovery with T2 turbo spin-echo. *Eur Radiol* 2006;16:1494–500